A new Methodology for achieving MMIC Bandpass Active Filters at High Frequencies

L. Darcel[1], P. Duême[1], R. Funck[1], G. Alquié[2]

[1]Thales Airborne Systems, 2 Av. Gay Lussac, 78851 Elancourt, France
Tel : +33 (0) 1 34 81 67 59, Email : laurence.darcel@fr.thalesgroup.com
[2]LISIF, University Pierre and Marie Curie, 4 place Jussieu, BP252, 75252 PARIS Cedex 05, France

Abstract — **This paper presents a new methodology based on actively coupled resonators, for achieving microwave active filters. In this method, which lends itself to narrowband and wideband filtering applications, we associate core cells with different resonance frequencies, adjusted separately, to synthesise a Butterworth, Chebyshev or other all-pole approximation. Two 1-pole bandpass filters centred at 9GHz, with 3dB bandwidth of 500 MHz, high gain of 17 dB and 21 dB, including a very low-noise active filter which exhibits a noise figure of 1.7 dB are realised in a first part. A 3-pole bandpass filter centred at 12GHz is also presented to validate this method, it has a gain of 15.5 dB ± 0.2 over a 1.5 GHz bandwidth and rejections better than 60 dB at 7 GHz and 18 GHz.**

I. Introduction

In RF and microwave systems, high volume passive filters are widely used. Integration of the filtering function, on an active MMIC, is an interesting way to save space. Although active filters have successfully been employed for many years at low frequencies, their design principles cannot be applied directly in the microwave region. If several authors have reported RF and microwave active narrowband filters for commercial telecommunication systems[1]-[2], a few of them were interested in wideband active filters for specialised military applications[3]-[4]. This paper presents a new methodology to achieve narrowband or wideband active filters fully integrated in MMIC technology. To demonstrate the practicability of the concept three active filters are presented. The first two are narrowband filters and demonstrate that this type of circuit can be associated with a low noise factor, which is one of the hardest point of the active technologies. The third circuit is a wideband filter (17% of 3 dB bandwidth).

II. CORE CELLS OF THE ACTIVE FILTERS

The filter synthesis technique presented below consists in *GLC* resonators coupled to each other through FETs. Because of the good unilaterality of this type of transistor, the input impedance depends weakly on the load impedance, so resonators can be treated separately at first approximation, and the circuit sensitivity to process variations is reduced .

The core cell shown in Fig. 1 is formed by the drain circuit of the input transistor, the *GpLpCp* parallel resonator and the gate circuit of the output transistor.

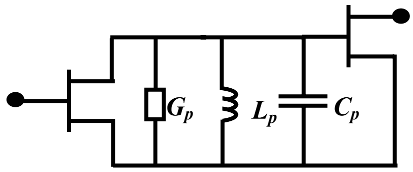

Fig. 1. Core cell of the active filters methodology.

The conductance *Gp* is included to take the losses of the cell into account and to control its Q-factor. This configuration has also the advantage that *Lp* can be used to bias the circuit. Fig. 2 shows the schematic of the equivalent circuit for the core cell, when the transistors are modelled as unilateral. The calculated attenuation function is given by:

$$A(\omega)=\frac{V_e}{V_s}=-\frac{1}{Gm}\cdot\left[G+\frac{R_g\cdot C_{gs}}{L_p}-R_g\cdot C\cdot C_{gs}\cdot\omega^2+j\cdot\frac{L_p\cdot\omega^2\cdot\left(C+C_{gs}\cdot(1+R_g\cdot G)\right)-1}{L_p\cdot\omega}\right] \quad (1)$$

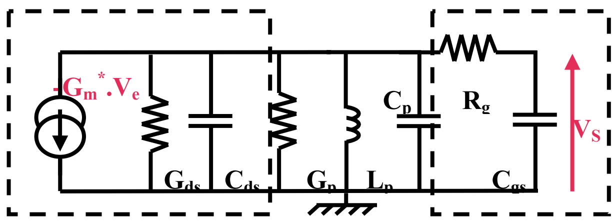

Fig. 2. Equivalent circuit of the core cell.

The approximate form of this function can be written as:

$$A(\omega)=A(\omega_0)\cdot\left[1+j\cdot Q\cdot\left(\frac{\omega}{\omega_0}-\frac{\omega_0}{\omega}\right)\right] \quad (2)$$

where Q is the quality factor of the cell and the resonant frequency (obtained when the attenuation is purely real). They are defined as:

$$\omega_0=\sqrt{\frac{1}{L_p\cdot\left(C+C_{gs}\cdot(1+R_g.G)\right)}} \quad (3)$$

$$Q=\frac{1}{L_p\cdot\omega_0\cdot\left[G+R_g\cdot C_{gs}^2\cdot(1+R_g\cdot G)\cdot\omega_0^2\right]} \quad (4)$$

Then the values of the resonator parameters can be expressed as functions of the FET equivalent circuit, w_0 and Q. To refine these equations, taking into account the non unilateral behaviour of the FETs, it is useful to introduce *Cgd* by applying the well-known Miller theorem.

III. SYNTHESIS PROCEDURE

The interest of the methodology presented in this paper is the possibility to synthesise a Butterworth, Chebyshev or other all-pole approximation from the core cell. In fact, a core cell with a resonance frequency of w_0 and a Q-factor of Q_0 has a pair of real poles, defined by:

$$p_1 = \pm \, {}^{1}\!/_{Q_0} \cdot w \tag{5}$$

where w is the normalised band of the required filter. But we have also two pairs of complex conjugate poles when two core cells are cascaded with the same Q and different frequencies w_{01} and w_{02}. In this case, we obtain:

$$p_2 = \frac{1}{2} \cdot \frac{\sqrt{w_0^2 + 4}}{Q \cdot w} + \frac{1}{2} \cdot j \cdot w_0 \cdot \frac{\sqrt{4 \cdot Q^2 - 1}}{Q \cdot w} \tag{6}$$

$$p_3 = -\frac{1}{2} \cdot \frac{\sqrt{w_0^2 + 4}}{Q \cdot w} + \frac{1}{2} \cdot j \cdot w_0 \cdot \frac{\sqrt{4 \cdot Q^2 - 1}}{Q \cdot w} \tag{7}$$

where $w_0 = \dfrac{\omega_{02} - \omega_{01}}{\omega_0}$

So it is possible, when the pole positions of the chosen approximation are calculated, to know the Q-factor and the resonance frequency of each core cell to achieve the desired filter. A n core cell active filter will contribute n pairs of transmission poles, as each stage will contribute one isolated pair. After this synthesis procedure, it is easy to derive the different values of the inductances, capacitances and resistors from equations (4-6).

III. DESIGN OF BANDPASS FILTERS

To illustrate the method presents the design of three GaAs MMIC active bandpass using the UMS PH25 (for the 1-pole filters) and PPH25 (for the 3-pole filter) processes (0.25 µm PHEMT technology). The design procedure of these three filters starts with a Chebyshev low-pass approximation, then the desired value of the conductance *Gp* is selected. So we can find the values of the inductors and capacitors with equations (4) and (5) for each core cell.

A. The 1-pole active bandpass filters

Two 1-pole active bandpass filters were realised, centred at 9 GHz. The first one (Fig. 3) is strictly using the active filter methodology but for the second one (Fig. 4), the core cell was modified to improve the noise figure. Both circuits are biased through the inductors.

The filters are matched to 50Ω at both ports using lumped L/C networks. To achieve a good isolation two 2×30 µm FETs are integrated. The layout of the first 1-pole filter is shown on Fig. 3. The overall chip dimensions are 1×1 mm^2, representing a very compact circuit.

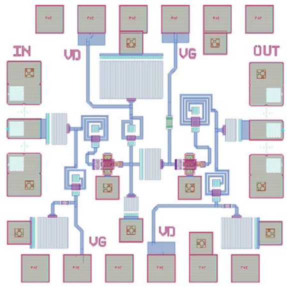

Fig. 3. Layout of the first 1-pole active filter.

Since active filters are intended to be used in receiver, they require high insertion gain but also low noise. Series feedback in the form of a small inductor introduced in the FET's source facilitates simultaneous gain and noise matching and in-band stability. In the case of the low-noise active filter, shown in Fig. 4, two 0.2 nH source inductors are placed. Chip size is 0.9×1.5 mm^2.

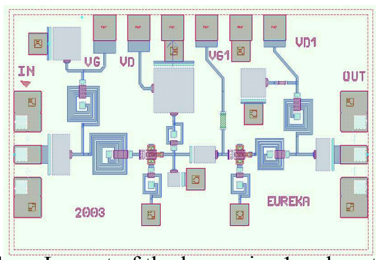

Fig. 4. Layout of the low-noise 1-pole active filter.

B. The 3-pole active bandpass filter

To realize a multi-stage bandpass filter with coupled resonators it is very important to isolate each cell. A single common-source FET cannot insure enough isolation in this case. Therefore we use a cascode configuration (a common-source FET followed by a common-gate FET) between the resonators.

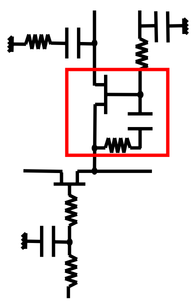

Fig. 5. Scheme of a common-gate FET biased by a saturated load

The first transistor of the bandpass filter is in a common-gate configuration, which is more unilateral at high frequencies and provides an active matching at the input. To improve the stability at low frequencies the drain of all the common-gate transistors are biased through a saturated load (a FET used as a current source) as shown in Fig. 5. The transistors used in the common-gate and cascode configurations are 2×40 µm devices and the FETs of the saturated load are 2×35 µm devices.

In order to reduce the size of the circuit and the number of parasitic elements, the FET of the saturated load and the common-gate transistors are laid out as a compact block, as shown on Fig. 6: the difference in gate width is clearly visible.

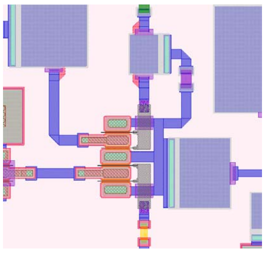

Fig. 6. Actively biased transistor.

The two fingers at the top belong to the transistor of the saturated load, and the two others to the common-gate FET. The input matching of the filter is realised by a common-gate FET (wideband active matching), the output matching uses L/C networks (a common-drain active matching is not stable enough).

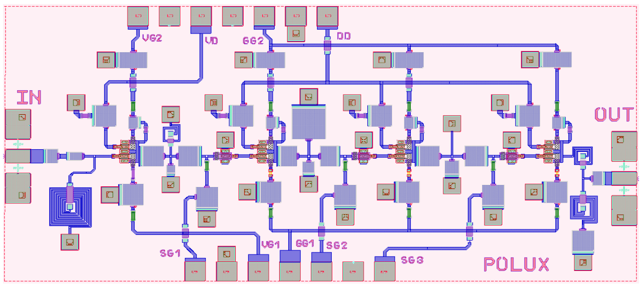

Fig. 7.Layout of the 3-pole active filter.

The 3-pole active filter, centred at 12 GHz, was synthesized by a Chebyshev formulation. Developing the resulting transfer function leads to a pair of real poles at 12 GHz and 2 pairs of complex conjugate poles at 11.4 GHz and 12.6 GHz. The three core cells are centered at different frequencies: the first one contributes to realize the pair of real poles at the center frequency and the two others contribute a pair of complex conjugate poles. Because of the low values of the inductances calculated for the 2nd and 3rd cells, narrow transmission lines shorted to ground through a via hole are implemented. The layout of the 3-poles filter is shown in Fig. 7. The overall chip dimensions are 3×1.4 mm^2.

IV. SIMULATION RESULTS

A. The 1-pole active bandpass filters

The simulated transfer characteristic of the two 1-pole filters are shown in Fig. 8 and 9 (low noise active filter). Both filters were defined with f_0= 9 GHz, w=0.015 and Lar=0.1 dB (where Lar is the maximum attenuation in the passe-band).

Both filters have an high insertion gain at 9 GHz, of 17 dB (filter #1) and 21 dB (filter #2), with a -3 dB bandwidth of 500 MHz, and rejection better than 17dB at ± 2.5 GHz from f_0. S_{11} and S_{22} are better than -20 dB for the filter #1, and than -15 dB for the filter #2. The low noise filter shows a noise figure of 1.7 dB over the band, which is a good result.

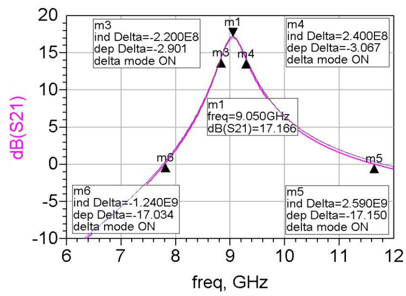

Fig. 8. Transfer characteristics of the first 1-pole filter.

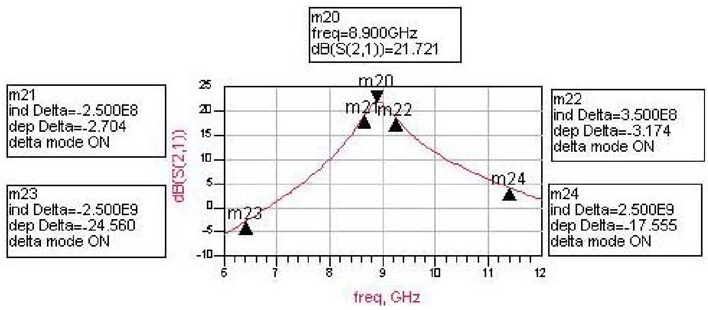

Fig. 9. Transfer characteristics of the first 1-pole filter (a) and of the low-noise 1-pole filter (b).

B. The 3-pole active bandpass filter

Fig. 10 shows the simulated transfer characteristic and S_{ii} of the multistage active filter. It has a gain of 15.3 dB ±0.2 over 12 GHz ±750 MHz bandwidth and rejections better than 60 dB at 7 Ghz and 18 GHz. $S_{11}$and S_{22} are better than -10 dB in all the band.

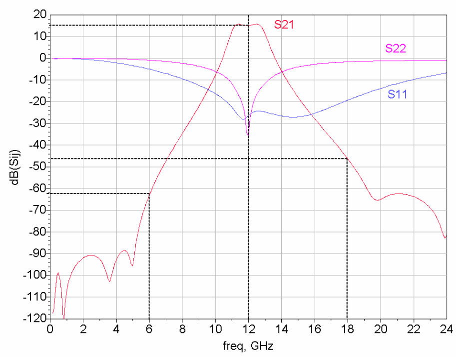

Fig. 10. Transfer characteristic and input/output return losses of the 3-pole active filter.

V. CONCLUSION

In this paper, a new methodology for achieving narrowband and wideband active filters at high frequencies is presented. The major advantages of this actively-coupled resonators methodology lies in its simplicity, small size, positive gain and the possibility to integrate other functions than the active filter on the MMIC chip. Because of its structure, it is less sensitive to the process variations, and can be realized as a low-noise function.

ACKNOWLEDGEMENT

The authors are thankful to C. Auric, B. Mallet-Guy and J-P. Plaze (Thales Airborne Systems) for their collaboration during this work.

REFERENCES

[1] F. Mahé, G. Tanné, E. Rius, C. Person, S.Toutain, F.Biron, L.Billonnet, B.Jarry, P. Guillon, "Electronically switchable dual-band microstrip interdigital bandpass filter multistandard communication applications", *EuMC 2000.*

[2] J.Vindevoghel , P. Descamps, "Narrowband active GaAs MMIC filters in K-band", *EuMC 2000.*

[3] C. Rauscher, "Two-branch microwave channelized active bandpass filters" , *IEEE Transactions on microwave theory and techniques*, vol.48, n°3, March 2000.

[4] R. Malmqvist, A. Gustafsson, M. Alfresson, A. Ouacha, "A tunable active MMIC filter for on-chip X-band radar receiver front-ends", *IEEE MTT-S 2002* pp.1907- 1910.